

Involvement of A5/a7 Noradrenergic Neurons and B2 Serotonergic Neurons in Nociceptive Processing: A Fiber Photometry Study

Shunpei Moriya (✉ msmr9040psyg80@gmail.com)

Kagoshima University Graduate School of Medical and Dental Science <https://orcid.org/0000-0002-2242-8214>

Akira Yamashita

Kagoshima Daigaku

Daiki Masukawa

Yokohama Shiritsu Daigaku

Junichi Sakaguchi

Kagoshima Daigaku

Honami Setoyama

Kagoshima Daigaku

Yoko Ikoma

Kagoshima Daigaku

Akihiro Yamanaka

Nagoya Daigaku

Tomoyuki Kuwaki

Kagoshima Daigaku

Short report

Keywords: nociception, A5 NA neurons, A7 NA neurons, B25-HT neurons, fiber photometry, G-CaMP6, mCherry, DBH-tTA mice, TPH-tTA mice

Posted Date: June 1st, 2020

DOI: <https://doi.org/10.21203/rs.3.rs-31869/v1>

License:   This work is licensed under a Creative Commons Attribution 4.0 International License.

[Read Full License](#)

Version of Record: A version of this preprint was published at Neural Regeneration Research on January 1st, 2022. See the published version at <https://doi.org/10.4103/1673-5374.322465>.

Abstract

In nociceptive processing, the descending antinociceptive system (DAS) is well known to include a number of descending pathways. As the main pathway of DAS, the locus coeruleus (A6) – spinal horn circuit including the noradrenergic (NAergic) system and the periaqueductal gray-rostral ventromedial medulla (B3) – spinal horn circuit including the serotonergic (5-HTergic) system are well known. Other NAergic or 5-HTergic systems, however, are less well known. Some studies have reported that A5/A7 noradrenaline (NA) neurons or B2 serotonin (5-HT, 5-hydroxytryptamine) neurons partially participate in DAS. In this study, we recorded G-CaMP6 green fluorescence signal intensities in the A5/A7/B2 sites of awake mice in response to acute tail pinch stimuli, acute heat stimuli, and in the context of a noninvasive control test, using fiber photometry with a calcium imaging system. We first introduced G-CaMP6 in the A5/A7 NA neuronal soma or B2 5-HT neuronal soma, using transgenic mice carrying tetracycline-controlled transactivator transgene (tTA) under the control of either a dopamine β -hydroxylase promoter or a tryptophan hydroxylase-2 and by the site-specific injection of adeno-associated virus (AAV-TetO(3G)-G-CaMP6). The specific expression patterns of G-CaMP6 were clearly confirmed in the A5/A7 areas and B2 area. After confirming the specific expression patterns of G-CaMP6, we recorded G-CaMP6 green fluorescence signals in these sites from awake mice in response to acute nociceptive stimuli. G-CaMP6 fluorescence intensity in the A5, A7, and B2 groups was rapidly increased by acute nociceptive stimuli, soon returning to baseline fluorescence intensity. This was not observed in the context of the noninvasive control test. We used mCherry red fluorescent protein as a control indicator. mCherry fluorescence intensity was not significantly changed by acute nociceptive stimuli or in the noninvasive control test in any of the groups. These results clearly indicate that acute nociceptive stimuli rapidly increase the activities of A5/A7 NA neurons or B2 5-HT neurons, suggesting that A5/A7 NA neurons or B2 5-HT neurons play important roles in nociceptive processing in the central nervous system.

Introduction

In modern clinical practice, pain symptoms are one of the important symptoms that clinicians treat. Pain symptoms are frequently present themselves with various mental disorders as well as physical disorders and are sometimes difficult to treat [1]. Especially in the case of mental disorders, the pathogenic mechanisms underlying their onset are sometimes unclear. In the field of psychiatry, pain symptoms present themselves in the form of neuropathic pain [2], somatoform pain disorder [3], major depressive disorder [4], and sleep-related disorder [5]. The monoaminergic system in the central nervous system (CNS) is thought to be involved in the etiology of these diseases [6, 7]. The role of monoaminergic signaling in nociceptive processing in the CNS is well known. In the pain management system, there are some descending pathways termed the descending antinociceptive system (DAS) [8, 9]. As the main pathways of the DAS, the locus coeruleus (LC, A6) – spinal horn circuit including the noradrenergic (NAergic) system and the periaqueductal gray (PAG)-rostral ventromedial medulla (RVM, B3) – spinal horn circuit including the serotonergic (5-HTergic) system are well known [10, 11]. Descending monoaminergic terminals are distributed in the spinal dorsal horn and regulate nociceptive signals. The NAergic system

has extensive innervation in the CNS, and subsets of noradrenaline (NE) cells are designed as A1-A7 groups in a caudal to rostral direction [12, 13]. The A6NE cell group is a well-recognized player in the DAS [10], while other NE cell groups are less well known. However, a few papers have reported that A5 and A7 NE cell groups are implicated in the regulation of antinociception [14, 15]. The A5 group is located in the ventrolateral part of the pons and the A7 group is located in the lateral part of the pons [16]. A5/A7 NE cells as well as A6 cells mainly project to the superficial spinal horn [16]. The 5-HTergic and NEergic systems have extensive innervations in the CNS, and subsets of serotonin (5-HT, 5-hydroxytryptamine) cells are identified as forming part of the B1–B9 group in a caudal to rostral direction [12]. The B3 5-HT group is a well-recognized player in the DAS, while other 5-HT cell groups are less well known [17]. The B2 (nucleus raphe obscurus) 5-HT cell group is located in the ventral part of medullary reticulum [18]. Unlike the B3 group, the B2 group mainly projects to the spinal intermediolateral cell column (IML) [19, 20] and spinal ventral horn [21]. The B2 group contributes to the regulation of autonomic function [19, 20] and motor function [20, 21]. To the best of our knowledge, few studies have assessed the contributing functions of the B2 group in the regulation of nociceptive processing. Recently, we reported that the activities of A6 NA neurons and B3 5-HT neurons in awake mice are rapidly increased in response to acute nociceptive stimuli using a fiber photometry system [22]. As aforementioned, a few studies have reported that A5/A7 NA neurons are implicated in the regulation of pain management, but to the best of our knowledge, only few studies have assessed how the activities of A5/A7 NA neurons are affected by nociceptive stimuli. A fiber photometry system adopting a calcium (Ca^{2+}) imaging system is an advanced tool for evaluating nociceptive signaling, as demonstrated in a recent paper focused on B9 5-HT neurons [23], A10 (ventral tegmental area, VTA) dopamine (DA) neurons [24], and A13 DA neurons [25]. Therefore, we deemed it meaningful to assess the activities of A5/A7 NA neurons and B2 5-HT neurons in response to acute nociceptive stimuli. We focused on these sites because these sites mainly form the descending pathways to the spinal cord.

We first introduced G-CaMP6 into A5/A7 NA neurons or B2 5-HT neurons using transgenic mice carrying tetracycline-controlled transactivator transgene (tTA) under the control of either a dopamine β -hydroxylase (DBH) promoter or a tryptophan hydroxylase-2 (TPH2), with a site-specific injection of an adeno-associated virus (AAV-TetO(3G)-G-CaMP6). After confirming the specific expression patterns of G-CaMP6 in the A5/A7 or B2 sites, we recorded the G-CaMP6 green fluorescence signal in these sites in awake mice in response to acute nociceptive stimuli.

Materials And Methods

Animals

We used transgenic mice carrying tTA under the control of a DBH or TPH2 promoter (DBH-tTA mice or TPH2-tTA mice, respectively) [22, 23, 24] (Fig. 1a); 10–14-week-old male mice were used in this experiment. Rearing was carried out in standard conditions, with lights on at 7:00 AM and off at 7:00 PM, at a temperature of $24 \pm 1^\circ\text{C}$, and food and water *ad libitum*. We made efforts to minimize animal affliction and reduce the

number of animals used. All experimental procedures were carried out in accordance with the National Institute of Health Guide for the Care and Use of laboratory Animals and approved by the Institutional Animal Use Committee of Kagoshima University (MD17105).

Stereotaxic AAV injection

Adeno-associated virus (AAV) vectors were produced using the AAV Helper-Free system (Agilent Technologies, Inc., Santa Clara, CA, USA) and purified as described previously [25]. AAV-TetO(3G)-G-CaMP6 (Serotype:DJ; 0.3 μ l/injection, 4×10^{13} copies/ml) and AAV-Tet(3G)-mCherry (Serotype:DJ; 0.3 μ l/injection, 6×10^{12} copies/ml) were produced using the Tet system (Fig. 1b). We slowly sucked up AAV into the glass micropipette (1B150F-3, World Precision Instruments, Inc., Sarasota, FL, USA) connected to an injection manipulator (I-200J, Narishige, Tokyo, Japan) linked to a nitrogen pressure source through polyethylene tubing. Under 2-3% isoflurane anesthetic conditions, mice were fixed with a stereotaxic instrument (ST-7, Narishige) with the help of supportive ear bar (EB-6, Narishige). To minimize suffering, the surfaces of their ears were covered with local anesthetic jelly (lidocaine, 2% xylocaine), and both eyes were preserved with vaseline. Head hair was shaved using an electric shaver and the cranial dura mater was cut open with small scissors. AAV was unilaterally injected into the target sites (A5: bregma -5.52mm, lateral +1.4mm, and ventral -5.30mm from the cranium; A7: bregma -4.96mm, lateral +1.88 mm, and ventral -3.10 mm from the surface of the brain; B2: bregma -7.56mm, and ventral -3.93mm from the cranium) (Fig. 1c) and the glass microtube was left in the sites for 10 minutes before being withdrawn. Postoperative antibiotic administration was carried out by a subcutaneous injection (penicillin G, 40,000 U kg^{-1}) to prevent postoperative infections. After the operation, mice were maintained in normal rearing conditions (see above) for 14 days (two weeks) to recover from the damage and to set aside a period allowing for the G-CaMP6/mCherry fluorescent protein to be fully expressed prior to the experimental sessions.

Immunohistochemistry

After the experiment, we performed immunohistochemistry to confirm the AAV-induced site-specific expression of G-CaMP6 and mCherry in mice. We transcardially perfused mice with 20ml of phosphate-buffered saline (PBS) and 20 ml of a 4% paraformaldehyde (PFA) solution under anesthesia with urethane (1.6 g/kg, ip). The brain was removed and post-fixed with 4% PFA and soaked in 30% sucrose in PBS for two days. We created a series of 30 μ m slices including the target sites with the cryostat (Cryotome FSE, Thermo Scientific, Yokohama, Japan) and immersed the sections in PBS for 24 hours at 4°C. Every third section was used for analysis. We washed the sections with PBS three times and incubated the sections with primary antibodies overnight. We diluted primary antibodies in blocking buffer and set the concentration as follows: A5/A7; anti-Tyrosine Hydroxylase raised in rabbit antibody (AB152, EMD Millipore Corp., Temecula, CA, USA) at 1:500, B2; anti-TPH antibody (AB1541, EMD Millipore Corp.) at 1:1000. The next day, we washed the sections with PBS three times and incubated the sections

with secondary antibodies at room temperature for two hours. We diluted secondary antibodies in PBS and set the concentration as follows; A5/A7: CF647 donkey anti-rabbit (20047, Biotium Inc., Fremont, CA, USA) in PBS at 1:200; B2: CF647 donkey anti-sheep (20284, Biotium Inc.) in PBS at 1:200. Next, we washed the sections with PBS once and mounted them on microscope slides (PRO-02, Matsunami, Osaka, Japan) and covered them with a micro cover glass (C024601, Matsunami). We observed the sections under a fluorescence microscope (BZ-X700, Keyence, Osaka, Japan), and created images using Adobe Photoshop CC software (Adobe Systems Inc., San Jose, CA, USA).

***In vivo* fiber photometry system**

In this study, we used the same fiber photometry system with two channels that we used in previous papers [22, 23, 24, 25]. We portray the scheme of the fiber photometry system (Fig. 2a). In brief, a high-power LED driver (LEDD1B/M470F3, Thorlabs Inc., Newton, NJ, USA) generates an excitation blue light (470nm, 0.5mW at the tip of the silica fiber) or yellow light (590nm) and the blue or yellow lights pass the excitation bandpass filter (blue light: pass 475 ± 12.5 nm; yellow light: 590 ± 12.5 nm) and are reflected by a dichroic mirror-1 and joined into the single silica fiber (diameter: 400 μ m, numerical aperture = 0.6). Blue/yellow lights emitted from the tip of the silica fiber reflect G-CaMP6/mCherry fluorescent proteins and green/red fluorescence signals are detected and transmitted to the same tube. The signals pass the dichroic mirror-1 and are reflected by a dichroic mirror-2 and pass the bandpass emission filter (green: pass 510 ± 12.5 nm; red: 607 ± 12.5 nm). At the end of the line, the signals are guided to a photomultiplier tube (PMT) (PMT-HS1-1P28, Zolix Instruments, Beijing, China). The signals were digitized by an A/D converter (PowerLab8/35, ADInstruments Inc., Dunedin, New Zealand) and recorded by Labchart version-7 software (ADInstruments Inc.).

Experimental protocol

In this study, we divided experimental mice into three groups: the A5, A7, and B2 groups. Fourteen days prior to recording, AAV was unilaterally injected into A5/A7 regions in DBH-tTA mice and B2 regions in TPH2-tTA mice (Fig. 1c). Each mouse was individually kept in normal breeding conditions for 14 days after the operation. In this study, we recorded the G-CaMP6/mCherry green/red fluorescence intensity of A5/A7 NA neuronal cell bodies and B2 5-HT neuronal cell bodies in response to acute nociceptive stimuli. Each of the four stimuli was presented once to each mouse (Fig. 2b). We applied an acute tail pinch stimulus at a force of 400 g using a pinch meter (PM-201, Soshin-Medic, Chiba, Japan) and an acute heat stimulus at a temperature of 55°C using a heating probe (5R7-570, Oven Industries Inc., Mechanicsburg, PA, USA) as per previous reports [23, 25]. As noninvasive control stimuli, we applied a gentle touch using a cotton stick and a low temperature stimulus corresponding to a temperature of 25°C using the same heating probe (5R7-570, Oven Industries Inc.).

We carried out the recording according to the following procedure. Each mouse was anesthetized with 2–3% isoflurane using a vaporizer and fixed with a stereotaxic instrument (ST-7, Narishige) using a

supportive ear bar (EB-6, Narishige). Surfaces of the ears were covered with a local anesthetic jelly (lidocaine, 2% xylocaine) to minimize suffering. We then carried out the silica fiber implantation operation. The silica fiber was placed just above the A5 site (bregma -5.52mm, lateral +1.4mm, and ventral -5.30mm from the cranium), A7 site (bregma -4.96mm, lateral +1.88 mm, and ventral -3.10 mm from the surface of the brain) and B2 site (bregma -7.56mm, and ventral -3.93mm from the cranium). We implanted the silica fiber slowly while monitoring the fluorescence signal intensity and confirmed that the fluorescence intensity increased rapidly when the optical position approached the target sites (Fig. 2c). After implantation, we ceased the administration of anesthesia. We waited for two hours after ceasing anesthesia until the first stimulus to reduce any possible effects of anesthesia. To reduce any possible effects of a previous stimulus, we set the inter-stimulus interval to 30 minutes and the order of stimuli as follows: the first was the low heat stimulus (25°C), the second was the gentle touch, the third was the heat stimulus (55°C) and the last was the pinch stimulus (Fig. 2b). We used the pinch meter (PM-201, Soshin-Medic) for the tail pinch stimulus and attached the apparatus to the root of the tail for three seconds with a force of 400g. We also used a heating probe (5R7-570, Oven Industries, Inc.) for the heat stimulus set to 55°C and attached the probe to the root of the tail for three seconds. For noninvasive control stimuli, we used a low heat stimulus using the same heat probe by touching the root of the tail for three seconds and by gently touching the mouse using a cotton stick at the root of the tail for three seconds.

We defined the neuronal activity characteristic index as follows: F: averaged fluorescence signal intensity value for three seconds immediately prior to each stimulus and defined as 100%; ΔF : maximum fluorescence signal intensity value during each stimulus - F; onset latency: time from the start of the stimulus to the time when the fluorescence signal intensity exceeded the maximum value during the baseline period; peak latency: time from the start of the stimulus to the maximum peak signal intensity.

Statistical analysis

Statistical analyses were conducted using a two-way analysis of variance (ANOVA) with the Sidak's test for post hoc analyses. The two factors of $\Delta F/F$ were the stimulus style (mechanical vs thermal) and stimulus intensity (nociceptive vs control). The two factors of onset/peak latency were the stimulus style (pinch vs heat) and target sites (A5 vs A7 vs B2). Data values were expressed as the mean \pm standard error of the mean (S.E.M). Probability values of $p < 0.05$ were considered statistically significant. Analyses were performed using GraphPad Prism version 7 (GraphPad software, San Diego, CA, USA).

Results

Expression patterns of AAV-induced G-CaMP6/mCherry

The specific expression patterns of G-CaMP6/mCherry were confirmed in A5/A7 NA neuronal soma (Fig. 3a, b) and B2 5-HT neuronal soma (Fig. 3c). G-CaMP6/mCherry-positive neurons were hardly observed

outside the A5, A7, and B2 areas. TH-positive cells were found in the A5 and A7 areas. A large proportion of them expressed G-CaMP6 (A5 area: 90.6%, A7 area: 90.9%) ($n = 6$, each) (Fig. 3d, e). All G-CaMP6 positive cells expressed mCherry, and a large proportion of them expressed TH (A5 area: 97.0%, A7 area: 85.7%) (Fig. 3d, e). TPH-positive cells were found in the B2 area. A large proportion of them expressed G-CaMP6 (91.8%) ($n = 6$, each) (Fig. 3f), and all G-CaMP6-positive cells expressed mCherry, while 94.3% expressed TPH (Fig. 3f). Therefore, green/red fluorescence was confirmed to be derived from specific A5/A7/B2 sites.

Effects of acute nociceptive stimuli on G-CaMP6/mCherry fluorescence intensity

We histologically confirmed that the fiber was properly positioned (see Additional file 1: Figure S1). G-CaMP6/mCherry fluorescence intensity were abruptly increased when the optical position was just above the target sites (Fig. 2c). Figure 4 shows the averaged traces of G-CaMP6/mCherry fluorescence intensity in response to acute nociceptive stimuli or a noninvasive control test ($n = 6$, each) (Fig. 4a-d). A two-way factorial ANOVA revealed that G-CaMP6 fluorescence intensity was significantly different across stimulus intensities (A5 group: pinch vs touch: $F(1, 5) = 36.84$, $p = 0.0018$, heat vs low heat: $F(1, 5) = 24.28$, $p = 0.0044$; A7 group: pinch vs touch: $F(1, 5) = 12.36$, $p = 0.0170$, heat vs low heat: $F(1, 5) = 11.48$, $p = 0.0195$; B2 group: pinch vs touch: $F(1, 5) = 50.10$, $p = 0.0009$, heat vs low heat: $F(1, 5) = 23.81$, $p = 0.0046$). An ANOVA revealed no significant difference in the onset/peak latency values across stimulus intensities (onset latency: pinch vs touch: $F(2, 10) = 0.3465$, $p = 0.7153$; heat vs low heat: $F(2, 10) = 0.1266$, $p = 0.8825$; peak latency: pinch vs touch: $F(2, 10) = 0.4141$, $p = 0.6718$; heat vs low heat: $F(2, 10) = 0.1148$, $p = 0.8927$). A two-way factorial ANOVA revealed that mCherry fluorescence intensity was not significantly different across stimulus intensities (A5 group: pinch vs touch: $F(1, 5) = 0.3742$, $p = 0.5675$, heat vs low heat: $F(1, 5) = 1.0350$, $p = 0.3557$; A7 group: pinch vs touch: $F(1, 5) = 0.3585$, $p = 0.5755$, heat vs low heat: $F(1, 5) = 0.0225$, $p = 0.8867$; B2 group: pinch vs touch: $F(1, 5) = 0.0014$, $p = 0.9719$, heat vs low heat: $F(1, 5) = 0.3598$, $p = 0.5747$).

The fluctuation in fluorescence intensity during the baseline period was as follows; G-CaMP6: A5 group ($0.67 \pm 0.14\%$), A7 group ($0.68 \pm 0.15\%$), B2 group ($0.62 \pm 0.14\%$), mCherry: A5 group ($0.74 \pm 0.11\%$), A7 group ($0.53 \pm 0.12\%$), B2 group ($0.51 \pm 0.11\%$). G-CaMP6 fluorescence intensity in all groups was rapidly increased by acute nociceptive stimuli but not by a noninvasive control test ($\Delta F/F$ values; A5 group: pinch/touch = $7.98 \pm 1.07/0.91 \pm 0.12$, $p < 0.001$, $55^\circ\text{C}/25^\circ\text{C} = 7.22 \pm 1.41/0.98 \pm 0.22$, $p < 0.001$; A7 group: pinch/touch = $8.20 \pm 2.16/0.68 \pm 0.22$, $p = 0.0018$, $55^\circ\text{C}/25^\circ\text{C} = 6.63 \pm 1.84/0.71 \pm 0.19$, $p = 0.014$; B2 group: pinch/touch = $7.97 \pm 0.89/0.70 \pm 0.19$, $p < 0.001$, $55^\circ\text{C}/25^\circ\text{C} = 9.00 \pm 1.56/0.74 \pm 0.27$, $p < 0.001$, $n = 6$, by a Sidak's test. mCherry fluorescence intensity in all groups was not significantly modified by any stimuli ($\Delta F/F$ values; A5 group: pinch/gentle = $0.59 \pm 0.13/0.70 \pm 0.11$, $55^\circ\text{C}/25^\circ\text{C} = 0.70 \pm 0.13/0.89 \pm 0.10$; A7 group: pinch/gentle = $0.79 \pm 0.26/0.61 \pm 0.19$, $55^\circ\text{C}/25^\circ\text{C} = 0.52 \pm 0.11/0.51 \pm 0.16$; B2 group: pinch/gentle = $0.62 \pm 0.13/0.61 \pm 0.16$, $55^\circ\text{C}/25^\circ\text{C} = 0.76 \pm 0.12/0.63 \pm 0.18$, $n = 6$, by Sidak's test. The response patterns to a tail pinch and heat stimuli in all groups were not significantly different, as shown by the statistical results of the onset and peak latencies ($p > 0.05$, by Sidak's test) (Fig. 5b, c).

Discussion

Our study clearly showed that the activities of A5/A7 NA neurons or B2 5-HT neurons were rapidly increased by acute nociceptive stimuli but not by a noninvasive control test. As mentioned earlier, A5 NA neurons are located in the ventrolateral pons and A7 NA neurons are located in the lateral part of the pons, with A5/A7 NA neurons projecting to the spinal cord and forming part of the pontospinal NAergic system [16]. The neuronal population of the NAergic DAS comprised about 80% A6 NA neurons, 12% A5 NA neurons, and 8% A7 neurons [26]. A few studies have demonstrated that the activation of A5 NA neurons appears to be chemically induced in conditions of pain [27, 28]. Martins et al. reported that pCREB expression was significantly increased in the A5 site of spinal nerve injury animals [29]. Another study reported that the A5-spinal pathway increased noxious-evoked c-fos expression [30]. These findings are consistent with our data.

A few studies have also reported that the chemical [31, 32, 33] or electrical [34] stimulation of A7 NA neurons regulates nociceptive processing. Few studies have assessed the physiological state of A7 NA cells. To the best of our knowledge, our study using a fiber photometry system is the first study to assess the activities of A5/A7 NA neuronal soma in response to nociceptive stimuli using electrophysiological methods. Our data clearly show a momentary reaction of A5/A7 and lay forth a new perspective with regard to the DAS.

With regard to the onset latency/peak latency, A5/A7 NA neurons did not show any significant differences, meaning that their response patterns of A5/A7 NA neurons did not depend on the types of stimuli. In a previous study, we showed that acute nociceptive stimuli rapidly increased the activity of A6 NA neurons in awake mice in real time conditions using a fiber photometry system [22]. In this study, the onset latency/peak latency values in the A6 site were as follows: pinch group, $0.4 \pm 0.2/1.9 \pm 0.3$, heat group, $0.7 \pm 0.1/3.5 \pm 0.7$. Given our data, it may be that A5/A6/A7 NA neurons nearly simultaneously react to acute nociceptive stimuli. In the future, studies comparing these characteristics in the same experimental system will be of interest. In addition, it may be that the LC-spinal NAergic system (A6 related) and pontospinal system (A5/A7 related) work nearly simultaneously in response to acute nociceptive processing. Wei et al. reported that A7 NA neurons affected A6 NA neurons by projecting their neuronal axons to the A6 area and regulating pain sensitivity [33]. Taking these findings into consideration, our data suggest that the A7-spinal NAergic pathway, A6-spinal NAergic pathway and A7-A6 NAergic pathway might influence each other. Studies investigating these possibilities will be needed in the future.

B2 5-HT neurons are little understood in the context of nociceptive processing. As mentioned in the Introduction, B2 5-HT neurons hardly project to the spinal dorsal horn, mainly targeting the IML [19, 20] or spinal ventral horn [21], and regulate autonomic function [19, 20] or motor function [20, 21]. To the best of our knowledge, our study is first study to assess the activities of B2 5-HT neurons by an electrophysiological method. Our data clearly showed that B2 5-HT neurons were implicated in

nociceptive processing. The IML or spinal ventral horn, like B2, are not well understood in the context of nociceptive processing. In addition to the DAS, the B2-IML/spinal 5-HTergic pathway may be implicated in nociceptive processing. Studies assessing this will be of interest in the future.

In a previous study, we confirmed that the activities of B3 5-HT neurons were rapidly increased by acute nociceptive stimuli [22]. Some electrophysiological studies have pointed to the activation of B3 5-HT neurons in response to nociceptive stimuli [35, 36]. As with A5/A7 parts, B2 parts did not show significant differences in the onset latency/peak latency, meaning that the response patterns of B2 5-HT neurons did not depend on the types of stimuli. In our previous paper, onset latency/peak latency values in B3 were as follows: pinch group, $0.5 \pm 0.1/2.4 \pm 0.5$, heat group, $1.8 \pm 1.0/5.2 \pm 1.8$) [22]. It may be that B2/B3 5-HT neurons nearly simultaneously react to acute nociceptive stimuli. Future studies assessing this will be of interest. Our present results provide new evidence of descending 5-HTergic nociceptive processing.

In this study, we used a fiber photometry system using G-CaMP6/mCherry proteins as intracellular calcium ion indicators. This calcium imaging system enables a high temporal resolution and is not affected by time lag and metabolism, differing as such from other electrophysiological and chemical methods. Therefore, our results are robust in that they are the product of momentary and non-medicated data.

In psychiatric clinical medicine, antidepressants are frequently prescribed for pain symptoms. Among antidepressants, serotonin noradrenaline reuptake inhibitors (SNRIs) are the most frequently prescribed. SNRIs mainly act on the synapses of NA neurons in the CNS and take at least a few weeks to improve pain symptoms [37]. Some studies have suggested that SNRIs inhibit the transmission of nociceptive information [38, 39]. In theory, a few weeks after starting to take SNRIs, the amount of NA in A5-A7 synapses is increased. This may affect the activities of A5/A7 NA neurons. Alongside SNRIs, selective serotonin reuptake inhibitors (SSRIs) or tricyclic antidepressants are also frequently prescribed. SSRIs mainly act on the synapses of 5-HT neurons in the CNS and affect the amount of 5-HT. This may affect the activities of B1/B2 5-HT neurons. We suggest that A5/A7/B2 neurons may represent new therapeutic targets.

There are some limitations to this study. We did not use SNRI/SSRI drugs and therefore did not assess how these drugs affect the activities of A5/A7 NA neurons or B2 5-HT neurons. We focused on nuclei origins located in the brain stem but not on the areas to which they project. In the future, the simultaneous measurement of neuronal activities in nuclei origins and spinal cord will be of acute interest. In addition, we used acute nociceptive stimuli rather than chronic nociceptive stimuli. In the future, studies using chronic stimuli will be needed.

In conclusion, acute nociceptive stimuli rapidly increased the activities of A5/A7 NA neurons or B2 5-HT neurons. This suggests that A5/A7 NA neurons or B2 5-HT neurons play important roles in nociceptive processing in the CNS.

Abbreviations

adeno-associated virus (AAV); central nervous system (CNS); descending antinociceptive system (DAS); dopamine (DA); dopamine β -hydroxylase (DBH); intermediolateral cell column (IML); locus coeruleus (LC); noradrenaline (NA); noradrenergic (NAergic); paraformaldehyde (PFA); periaqueductal gray (PAG); phosphate-buffered saline (PBS); photomultiplier tube (PMT); rostral ventromedial medulla (RVM); selective serotonin reuptake inhibitor (SSRI); serotonergic (5-HTergic); serotonin (5-HT, 5-hydroxytryptamine); serotonin noradrenaline reuptake inhibitor (SNRI); standard error of the mean (S.E.M); tetracycline-controlled transactivator transgene (tTA); tryptophan hydroxylase-2 (TPH2); ventral tegmental area (VTA)

Declarations

Acknowledgments

We thank all staff members of the Institute of Laboratory Animal Sciences at Kagoshima University for keeping the animals in good condition. We acknowledge the Joint Research Laboratory, Kagoshima University Graduate School of Medical and Dental Sciences, for the use of their facilities.

Authors' contributions

SM and TK designed the study. SM, A.Yamashita, JS, HS, and YI conducted the study with the supports of A.Yamanaka and TK. SM and DM analyzed the data and created the figure. SM and TK wrote the manuscript.

Funding

This work was supported by JSPS KAKENHI grants (19K17093 to SM; 20K06858 to A. Yamashita; 16H05130 to TK) and CREST JST (JPMJCR1656 to A. Yamanaka).

The authors have no conflicts of interest to declare.

Availability of data and material

The datasets analyzed in this study are available from the corresponding author upon request.

Ethics approval

All experimental procedures were carried out in accordance with the National Institute of Health Guide for the Care and Use of laboratory animals and approved by the institutional Animal Use Committee of

Consent for publication

Not applicable.

Competing interests

The authors declare that they have no competing interests.

References

1. Makris UE, Abrams RC, Gurland B, Reid MC. Management of persistent pain in the older patient: a clinical review. *JAMA*. 2014;312(8):825-36.
2. Attal N, Bouhassira D. Translational neuropathic pain research. *Pain*. 2019;160 Suppl1:S23-s8.
3. Waller E, Scheidt CE. Somatoform disorders as disorders of affect regulation: a development perspective. *Int Rev Psychiat*. (Abingdon, England). 2006;18(1):13-24.
4. Gebhardt S, Heinzl-Gutenbrunner M, Konig U. Pain relief in depressive disorders: a meta-analysis of the effects of antidepressants. *J Clin Psychopharmacol*. 2016;36(6):658-68.
5. Morin CM, Drake CL, Harvey AG, Krystal AD, Manber R, Riemann D, et al. Insomnia disorder. *Nat Rev Dis Primers*. 2015;1:15026.
6. Llorca-Torralba M, Borges G, Neto F, Mico JA, Berrocoso E. Noradrenergic locus coeruleus pathways in pain modulation. *Neuroscience*. 2016;338:93-113.
7. Nardone R, Holler Y, Thomschewski A, Holler P, Lochner P, Golaszewski S, et al. Serotonergic transmission after spinal cord injury. *J Neural Transmission* (Vienna, Austria: 1996). 2015;122(2):279-95.
8. Melzack R, Wall PD. 1965. Pain mechanisms: a new theory. *Science* (New York, NY). 1965;150(3699):971-9.
9. Millan MJ. Descending control of pain. 2002. *Prog in Neurobiol*. 2002;66(6):355-474.
10. Yaksh TL, Hammond DL, Tyce GM. Functional aspects of bulbospinal monoaminergic projections in modulating processing of somatosensory information. *Fed Proceed*. 1981;40(13):2786-94.
11. Ochi T, Goto T. The antinociceptive effect induced by FR140423 is mediated through spinal 5-HT_{2A} and 5-HT₃ receptors. *Eur J Pharmacol*. 2000;409(2):167-72.

12. Dahlstrom A, Fuxe K. Localization of monoamines in the lower brain stem. *Experientia*. 1964;20(7):398-9.
13. Pertovaara A. Noradrenergic pain modulation. *Prog in Neurobiol*. 2006;80(2):53-83.
14. Mravec B, Bodnar I, Uherezky G, Kvetnansky R, Palkovits M. Effect of lesions of A5 or A7 noradrenergic cell group or surgical transection of brainstem catecholamine pathways on plasma catecholamine levels in rats injected subcutaneously by formalin. *Gen Physiol and Biophysics*. 2012;31(3):247-54.
15. Nuseir K, Proudfit HK. Bidirectional modulation of nociception by GABA neurons in the dorsolateral pontine tegmentum that tonically inhibit spinally projecting noradrenergic A7 neurons. *Neuroscience*. 2000;96(4):773-83.
16. Proudfit HK, Clark FM. The projections of locus coeruleus neurons to the spinal cord. *Prog in Brain Res*. 1991;88:123-41.
17. Jacobs BL, Azmitia EC. Structure and function of the brain serotonin system. *Physiological Rev*. 1992;72(1):165-229.
18. Jacobs BL, Martin-Cora FJ, Fornal CA. Activity of medullary serotonergic neurons in freely moving animals. *Brain Res Rev*. 2002;40(1-3):45-52.
19. Allen GV, Cechetto DF. Serotonergic and nonserotonergic neurons in the medullary raphe system have axon collateral projections to autonomic and somatic cell groups in the medulla and spinal cord. *J Comp Neurol*. 1994;350(3):357-66.
20. Benarroch EE. Medullary serotonergic system: organization, effects, and clinical correlations. *Neurology*. 2014;83(12):1104-11.
21. Saruhashi Y, Young W, Perkins R. The recovery of 5-HT immunoreactivity in lumbosacral spinal cord and locomotor function after thoracic hemisection. *Experimental Neurol*. 1996;139(2):203-13.
22. Moriya S, Yamashita A, Nishi R, Ikoma Y, Yamanaka A, Kuwaki T. Acute nociceptive stimuli rapidly induce the activity of serotonin and noradrenalin neurons in the brain stem of awake mice. *IBRO Rep*. 2019;7:1-9.
23. Moriya S, Yamashita A, Masukawa D, Kambe Y, Sakaguchi J, Setoyama H, et al. Involvement of suprallemniscal nucleus (B9) 5-HT neuronal system in nociceptive processing: a fiber photometry study. *Mol Brain*. 2020;13(1):14.
24. Moriya S, Yamashita A, Kawashima S, Nishi R, Yamanaka A, Kuwaki T. Acute aversive stimuli rapidly increase the activity of ventral tegmental area dopamine neurons in awake mice. *Neuroscience*. 2018;386:16-23.

25. Moriya S, Yamashita A, Masukawa D, Setoyama H, Hwang Y, Yamanaka A, et al. Involvement of A13 dopaminergic neurons located in the zona incerta in nociceptive processing: a fiber photometry study. *Mol Brain*. 2020;13(1):60.
26. Ikoma Y, Kusumoto-Yoshida I, Yamanaka A, Ootsuka Y, Kuwaki T. Inactivation of Serotonergic Neurons in the Rostral Medullary Raphe Attenuates Stress-Induced Tachypnea and Tachycardia in Mice. *Front in Physiol*. 2018;9:832.
27. Inutsuka A, Yamashita A, Chowdhury S, Nakai J, Ohkura M, Taguchi T, et al. The integrative role of orexin/hypocretin neurons in nociceptive perception and analgesic regulation. *Sci Rep*. 2016;6:29480.
28. Howorth PW, Teschemacher AG, Pickering AE. Retrograde adenoviral vector targeting of nociceptive pontospinal noradrenergic neurons in the rat in vivo. *J Comp Neurol*. 2009;512(2):141-57.
29. Tavares I, Lima D, Coimbra A. The pontine A5 noradrenergic cells which project to the spinal cord dorsal horn are reciprocally connected with the caudal ventrolateral medulla in the rat. *Eur J Neurosci*. 1997;9(11):2452-61.
30. Marques-Lopes J, Pinho D, Albino-Teixeira A, Tavares I. The hyperalgesic effects induced by the injection of angiotensin II into the caudal ventrolateral medulla are mediated by the pontine A5 noradrenergic cell group. *Brain Res*. 2010;1325:41-52.
31. Martins I, Carvalho P, de Vries MG, Teixeira-Pinto A, Wilson SP, Westerink BH, et al. Increased noradrenergic neurotransmission to a pain facilitatory area of the brain is implicated in facilitation of chronic pain. *Anesthesiology*. 2015;123(3):642-53.
32. Tavares, I., Lima, D. The caudal ventrolateral medulla as an important inhibitory modulator of pain transmission in the spinal cord. *J Pain*. 2002;3, 337-46.
33. Yeomans DC, Clark FM, Paice JA, Proudfit HK. Antinociception induced by electrical stimulation of spinally projecting noradrenergic neurons in the A7 catecholamine cell group of the rat. *Pain*. 1992;48(3):449-61.
34. Jeong Y, Moes JR, Wagner M, Holden JE. The posterior hypothalamus exerts opposing effects on nociception via the A7 catecholamine cell group in rats. *Neuroscience*. 2012;227:144-53.
35. Wei H, Pertovaara A. Regulation of neuropathic hypersensitivity by alpha (2) -adrenoceptors in the pontine A7 cell group. *Basic & Clin Pharmacol & Toxicol*. 2013;112(2):90-5.
36. 34. Yeomans DC, Proudfit HK. Antinociception induced by microinjection of substance P into the A7 catecholamine cell group in the rat. *Neuroscience*. 1992;49(3):681-91.
37. Wessendorf MW, Anderson EG. Single unit studies of identified bulbospinal serotonergic units. *Brain Res*. 1983;279(1-2):93-103.
38. Chiang CY, Gao B. The modification by systemic morphine of the responses of serotonergic and non-serotonergic neurons in nucleus raphe magnus to heating the tail. *Pain*. 1986;26(2):245-57.
39. Mitsi, V., Zaxhariou, V. Modulation of pain, nociception, and analgesia by the brain reward center. *Neuroscience*. 2016;338, 81-92.

40. Attal N. Neuropathic pain: mechanisms, therapeutic approach, and interpretation of clinical trials. *Continuum (Minneapolis, Minn)*. 2012;18(1):161-75.
41. Vranken JH. Elucidation of pathophysiology and treatment of neuropathic pain. *Cent Nerv Syst Agents Med Chem*. 2012;12(4):304-14.

Figures

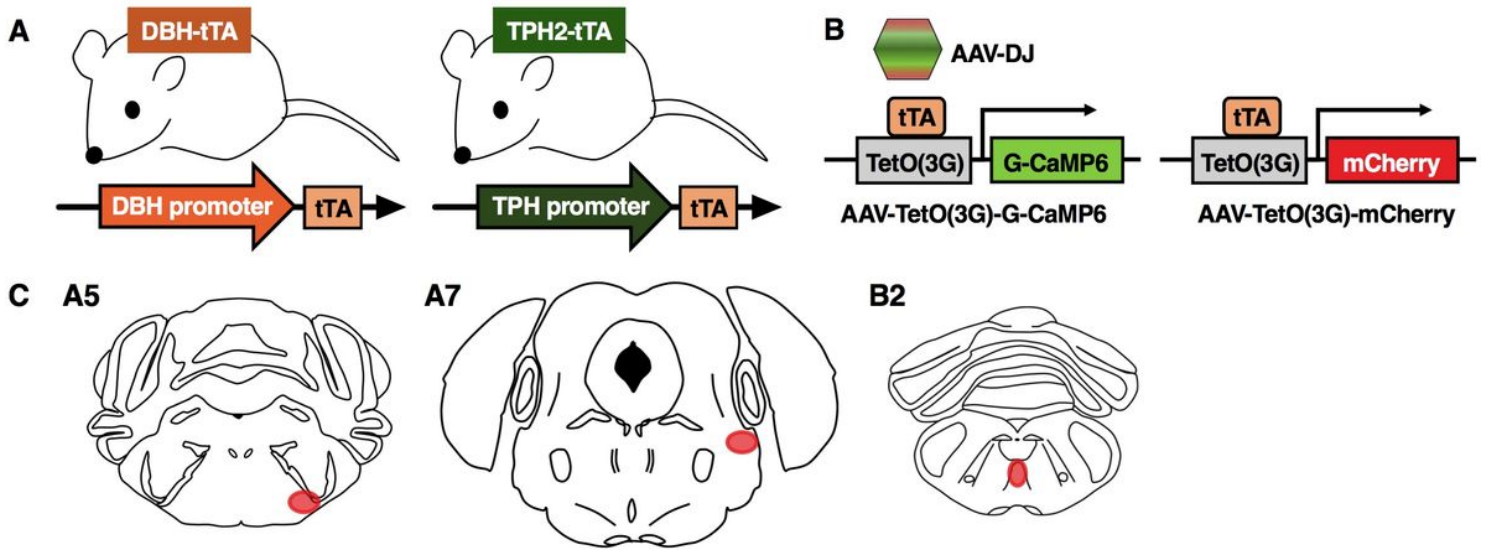


Figure 1

5-HT or NA neuron-specific expression patterns of G-CaMP6 or mCherry fluorescent proteins adopting Tet system. (a) genetic scheme of DBH-tTA mice or TPH2-tTA mice, carrying tTA under the control of DBH-tTA or TPH2 promoter. (b) G-CaMP6 and mCherry fluorescent proteins expressed using the tTA/TetO system. (c) AAV injection into the target sites (A5,A7 and B2).

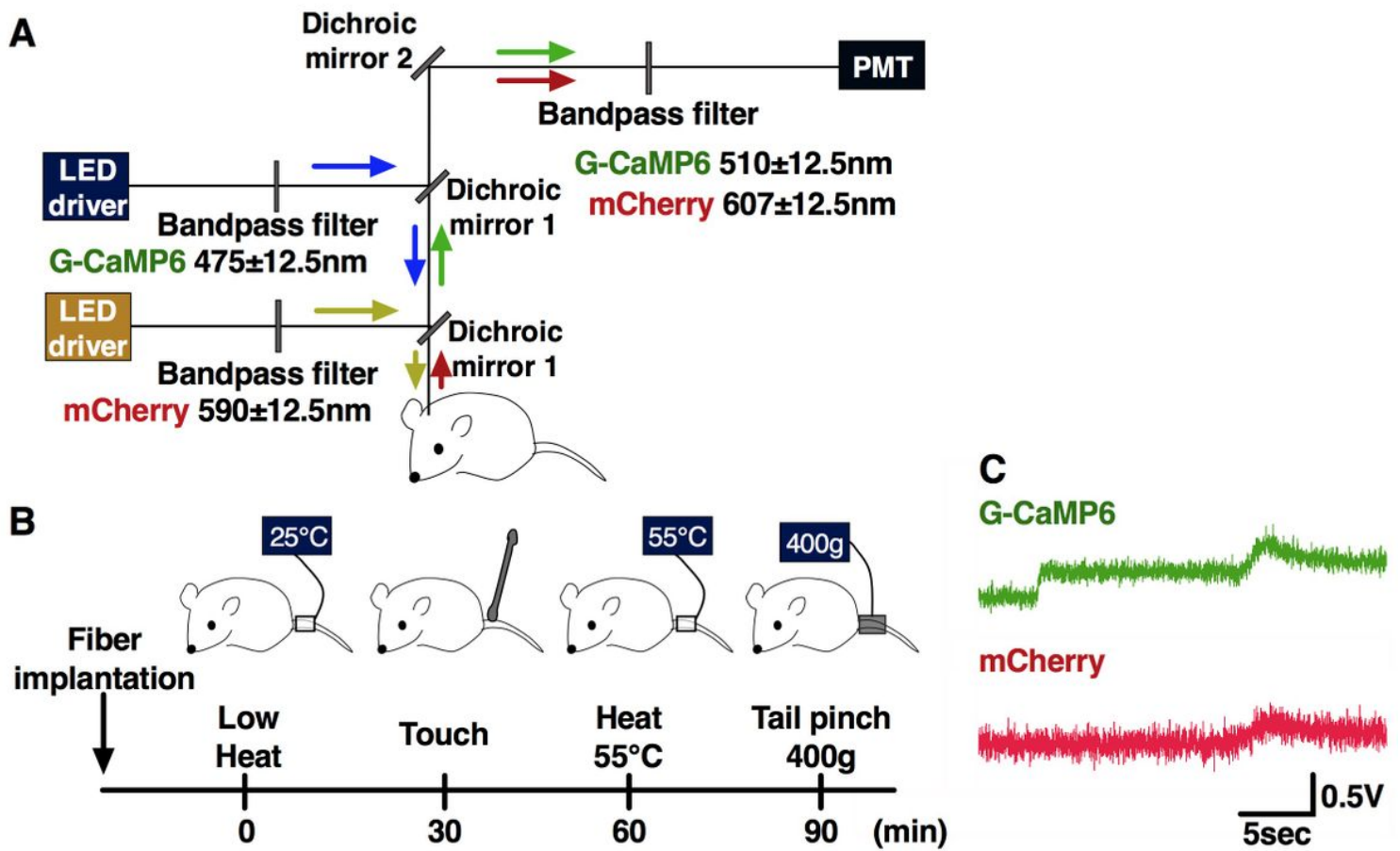


Figure 2

Experimental procedures. (a) Schematic representation of the fiber photometry system with two channels. (b) Recording procedure. Each of the four stimuli delivered once to each mouse. We set the inter-stimulus interval to be 30 minutes to reduce any possible effects of previous stimuli. (c) Monitoring of the fluorescence signal intensity. It is confirmed that the fluorescence intensity increased rapidly when the optical position approached the target sites.

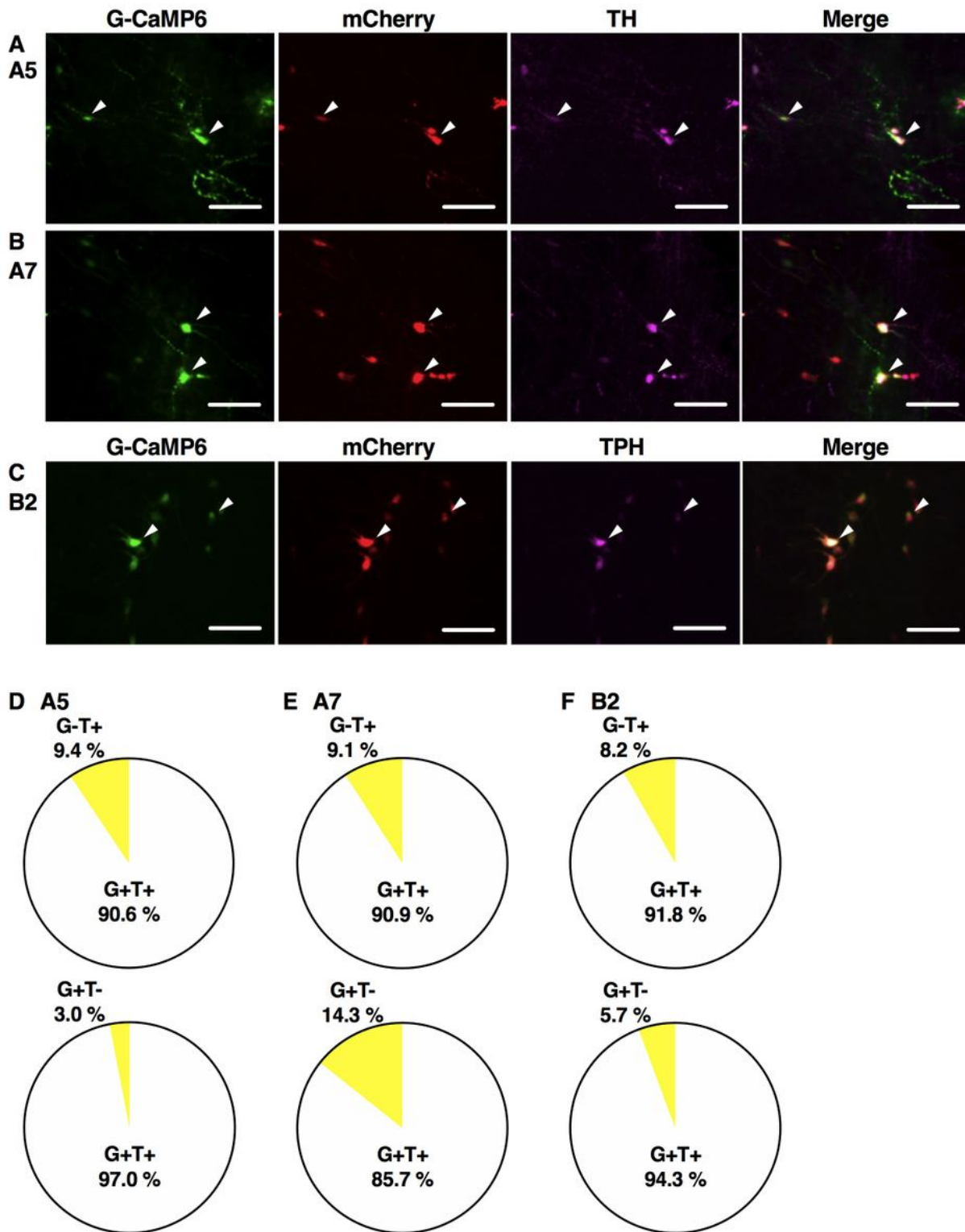


Figure 3

Expression of AAV-induced G-CaMP6/mCherry.(a – c)Specific expression patterns of G-CaMP6/mCherry confirmed in A5/A7 NA neuronal soma (white rectangles) (a, b) and B2 5-HT neuronal soma(white rectangles) (c).TH-positive cells found in the A5 and A7 areas (a, b).TPH-positive cells found in the B2 area (c). A large proportion of TH-positive cells expressed G-CaMP6 (A5 area: 90.6%, A7 area: 90.9%)(n = 6, each) (d, e).All G-CaMP6-positive cells expressed mCherry and a large proportion of them expressed TH

(A5 area: 97.0%, A7 area: 85.7%) (d, e). A large proportion of TPH-positive cells expressed G-CaMP6 (91.8%) (n = 6, each) (f). All G-CaMP6 positive cells expressed mCherry and 94.3% expressed TPH (f). Scale bar: 100 μ m.

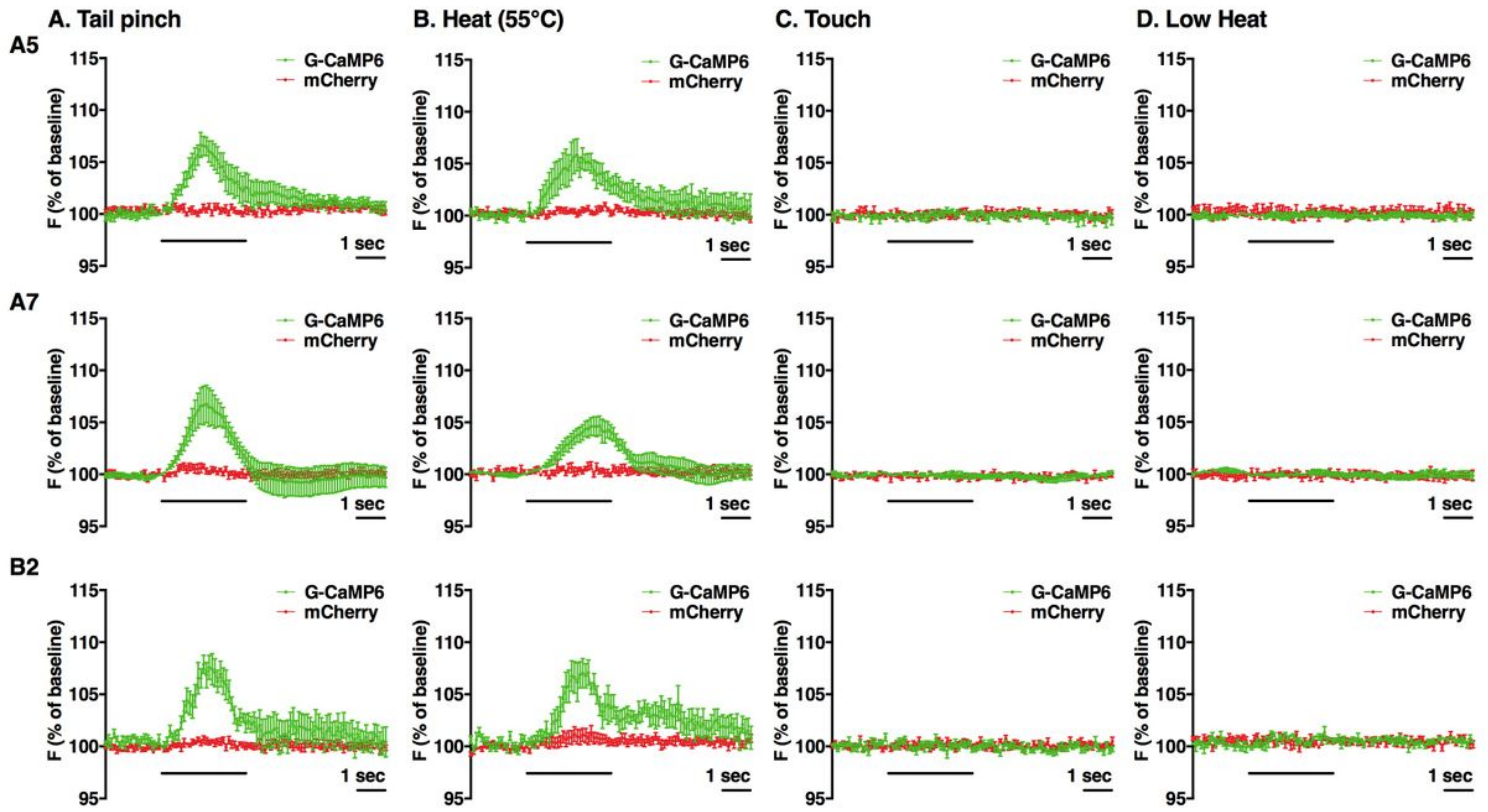


Figure 4

Averaged traces of G-CaMP6/mCherry (green/red) fluorescence intensity in response to stimuli. (a, b) acute nociceptive stimuli or (c, d) a noninvasive control test (n = 6, each). Brief scale bar: 1 sec; long scale bar: 3 sec.

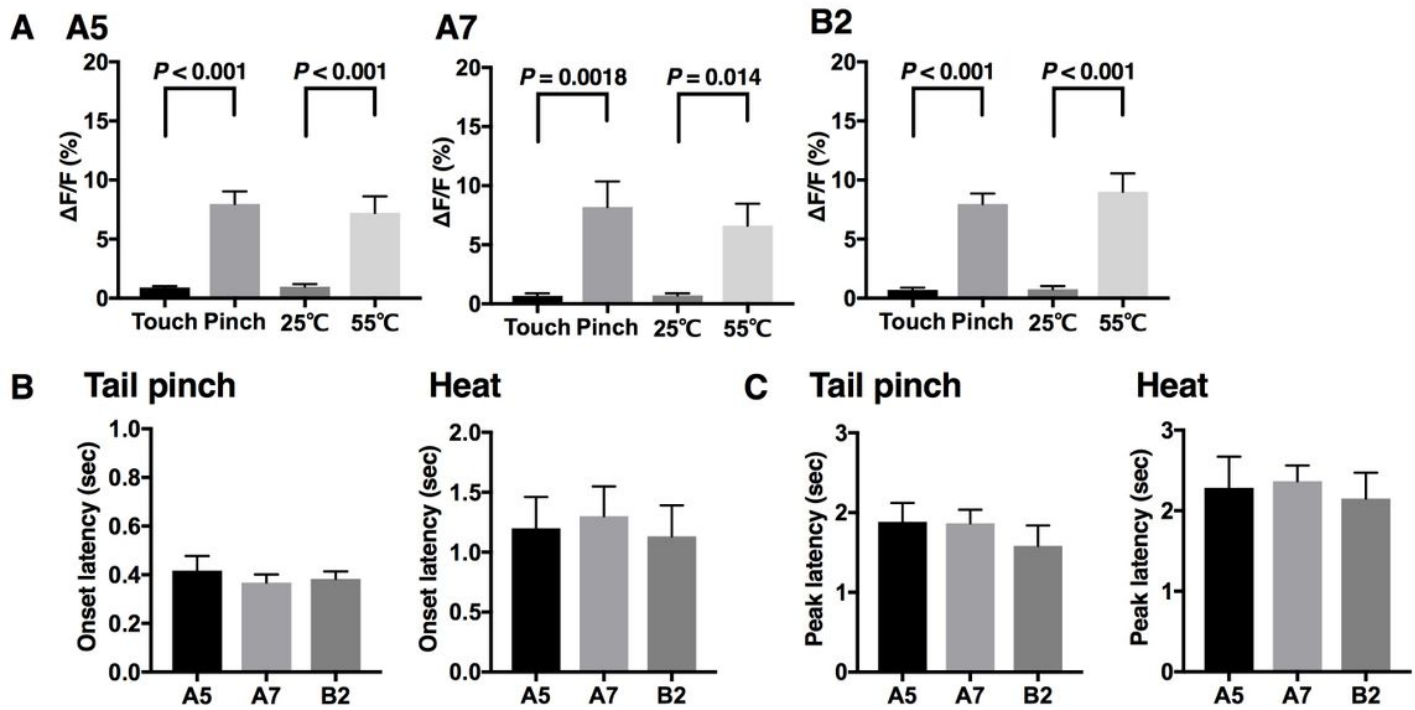


Figure 5

Effects of acute nociceptive stimuli or a noninvasive control test on G-CaMP6/mCherry fluorescence signals. (a) G-CaMP6 fluorescence intensity in all groups rapidly increased by acute nociceptive stimuli but not by a noninvasive control test. (b) The response pattern to a tail pinch and heat stimuli in all groups not significantly different, as indicated by the statistical results of the onset and peak latency values. Data are expressed as values of the mean \pm S.E.M and analyzed using a two-way ANOVA with the Sidak's test ($n = 6$, each). P values represent the statistical results of the Sidak's test.

Supplementary Files

This is a list of supplementary files associated with this preprint. Click to download.

- [renamedfc291.doc](#)
- [Supplementalfigure1.tiff](#)